Tracking individual secretory vesicles during exocytosis reveals an ordered and regulated process

Kirk W. Donovan and Anthony Bretscher

Department of Molecular Biology and Genetics, Weill Institute for Cell and Molecular Biology, Cornell University, Ithaca, NY 14853

Post-Golgi secretory vesicle trafficking is a coordinated process, with transport and regulatory mechanisms to ensure appropriate exocytosis. While the contributions of many individual regulatory proteins to this process are well studied, the timing and dependencies of events have not been defined. Here we track individual secretory vesicles and associated proteins in vivo during tethering and fusion in budding yeast. Secretory vesicles tether to the plasma membrane very reproducibly for ∼18 s, which is extended in cells defective for membrane fusion and significantly lengthened and more variable when GTP hydrolysis of the exocytic Rab is delayed. Further, the myosin-V Myo2p regulates the tethering time in a mechanism unrelated to its interaction with exocyst component Sec15p. Two-color imaging of tethered vesicles with Myo2p, the GEF Sec2p, and several exocyst components allowed us to document a timeline for yeast exocytosis in which Myo2p leaves 4 s before fusion, whereas Sec2p and all the components of the exocyst disperse coincident with fusion.

Introduction

The functional organization of eukaryotic cells is dependent on the faithful packaging of cargos into membrane-bound vesicles and their transport to and fusion with the appropriate membrane. Exocytosis is an essential process and allows a cell to secrete molecules and peptides, regulate the composition of its plasma membrane, and enable growth (Brennwald and Rossi, 2007); defects in specific steps can lead to severe human diseases and conditions including Charcot-Marie-Tooth syndrome and X-linked mental retardation (D'Adamo et al., 1998; Zhao et al., 2001). Budding yeast is an attractive model in which to study exocytosis due to the large collection of characterized mutants and well-established conservation of function in mammalian cells (Novick et al., 1980; Salminen and Novick, 1987; Liu and Bretscher, 1989; Johnston et al., 1991).

Post-Golgi secretory trafficking in yeast begins as secretory vesicles mature from the trans-Golgi network via Rab cascades and an unknown scission event (Ortiz et al., 2002). After the transition from Rab11 homologue Ypt31/32p to Rab8 homologue Sec4p, the exocyst tethering complex, through Sec15p, binds active Sec4-GTP (Guo et al., 1999). Transport-competent secretory vesicles then bind to and activate the myosin-V motor Myo2p, through direct binding to both Sec4-GTP and Sec15p (Jin et al., 2011; Santiago-Tirado et al., 2011; Donovan and Bretscher, 2012). Rapid polarized transport along formin-nucleated actin cables delivers secretory vesicles to sites of growth in the bud where the exocyst complex (Sec3p, Sec5p, Sec6p, Sec8p, Sec10p, Sec15p, Exo70p, and Exo84p) then engages to physically tether the vesicle to the plasma membrane (TerBush and Novick, 1995; Evangelista et al., 2002; Schott et al., 2002; Luo et al., 2014). Finally, regulatory interactions between exocyst components (Sivaram et al., 2005; Morgera et al., 2012), SNARE proteins (Lehman et al., 1999), GTPase activating proteins (GAPs; Gao et al., 2003), and SM proteins (Carr et al., 1999; Scott et al., 2004; Togneri et al., 2006) contribute to the final stage of exocytosis, vesicle fusion, though the timing and order of events is still undefined.

Here we present the first timeline of events for yeast exocytosis of individual secretory vesicles. We show that vesicles physically tether to the plasma membrane for a short period of time (∼18 s). Two-color imaging shows that the myosin-V motor Myo2p leaves the vesicle before fusion, but other components associated with vesicles, including the GEF Sec2p and the exocyst complex, leave the vesicle at the moment of fusion. Further, we reveal dependencies in this timeline by exploring how defects in Sec4-GTP hydrolysis, Myo2p motors, an SM protein, and exocyst components affect tethering and fusion. Given the conservation of this pathway in mammalian cells, these results are likely widely applicable.

Results and discussion

Individual secretory vesicle tethering and fusion events can be followed in vivo

Yeast cells contain ∼7,000 molecules of Sec4p, of which ∼4,000 molecules are present in a growing bud (Donovan and

Correspondence to Anthony Bretscher: apb5@cornell.edu

Abbreviations used in this paper: FLIP, fluorescence loss in photobleaching; GAP, GTPase activating protein.

The Rockefeller University Press $30.00
J. Cell Biol. Vol. 210 No. 2 181–189
www.jcb.org/cgi/doi/10.1083/jcb.201501118

Bretscher, 2012). Other proteins that are part of the exocytosis machinery are similarly well polarized, including components of the exocyst complex (TerBush and Novick, 1995), the myosin-V Myo2p (Lillie and Brown, 1994), and SNARE regulators Sec1p and Sro7/77p (Carr et al., 1999; Rossi and Brennwald, 2011). Using fluorescently tagged proteins, we previously documented the bulk population dynamics of secretory vesicles and associated proteins during exocytosis (Donovan and Bretscher, 2012). While individual secretory vesicles carrying fluorescently tagged proteins have been tracked in the mother cell for more than a decade (Schott et al., 2002; Boyd et al., 2004), they become challenging to follow once they enter the bud due to the highly polarized nature of the yeast secretory system. To circumvent this problem, we examined the feasibility of photobleaching all signal from secretory vesicles already in the bud to allow observation of new vesicles entering from the mother cell. Our goal is to determine a timeline of events for yeast exocytosis, and then explore how it is perturbed in mutant cells.

Control experiments showed that photobleaching the entire bud with a 488-nm laser did not affect the cell growth rate compared with unbleached cells, suggesting that the bleach event was not disturbing essential processes in exocytosis (Fig. S1 A). Wild-type cells containing chromosomally integrated *GFP-SEC4* as its sole copy were then subjected to vesicle tracking procedures. After bleaching a late-G2 phase bud of all signal, new vesicles arriving in the bud moved around too rapidly to follow easily; however, once they contact the cortex the vesicles remain stationary (what we will refer to as "tethering") and could be confidently tracked until the GFP-Sec4 signal suddenly disappeared in a rapid frame-to-frame event (Fig. 1 A).

To follow the tethering and disappearance events, we captured five focal planes, covering ∼2.5 µm, with a time resolution of ∼1.3 s per frame. To ensure that we are following the complete history of a vesicle's tethering, we only used data in which the initial tethering event was clearly seen and the disappearance event was only counted if it occurred in one of the three middle imaging planes. The stationary vesicles in these events invariably occurred at the cell cortex (Fig. S1 B). This disappearance event almost certainly represents vesicle fusion as we determined the diffusion rate of unextracted GFP-Sec4 in the plasma membrane in a mutant lacking the GAPs for Sec4p (Fig. S1 C). This rate was sufficiently fast to accommodate punctate GFP-Sec4 on a vesicle rapidly diffusing into the larger plasma membrane space during the disappearance event we observe. It is unlikely to be GDI extraction of Rabs on the vesicle because the puncta's complete disappearance (representing >50 Rab molecules; Donovan and Bretscher, 2012) occurs so quickly. Other methods to determine vesicle fusion, such as colocalization with a fluorescent cargo reporter or using a pH-sensitive variant, were attempted but proved difficult to use due to the folding rate of fluorescent proteins and the rapid nature of the yeast secretory system (only 8 min for some proteins; Novick and Schekman, 1983). Lastly, we are capturing individual secretory vesicles in this analysis, as the number of vesicles entering the bud per unit of time matches the expected rates of exocytosis of about one vesicle every 3 s, given the surface area of the vesicles and final bud, time of growth, and endocytosis rates (Donovan and Bretscher, 2012). Thus, we can track individual secretory vesicle tethering and fusion with the plasma membrane.

Vesicle tethering time is uniform and lengthened by delaying Rab GTP hydrolysis or inhibiting membrane fusion

We first sought to determine the length of time that vesicles are tethered to the cortex in wild-type cells. Their location after tethering was tracked in three dimensions, though for presentation purposes here we show maximum projection still frames or kymographs (Fig. 1, A and B). The tethering time at the cortex was remarkably consistent, with an average of 18.1 ± 4.2 s (n = 22; Fig. 1 C and Video 1), which suggests that a timed order of events regulates the tethering and fusion processes. This length of time also fits well with observed Myo2p motor recycling, as motors associated with secretory vesicles only reside in the bud for ∼30 s (which includes transit and recycling times; Donovan and Bretscher, 2012). Some vesicles used in this analysis were tracked near the distal end of the bud while others were tracked at the sides. As the bud is growing isotropically at this cell stage, it is not surprising that we did not detect a difference in tethering and fusion dynamics between these two populations (Fig. 1 C).

Having revealed the consistency in tethering time before fusion, we examined the consequence of delaying the critical Sec4-GTP hydrolysis event. The constitutively active Sec4-Q79L mutant shows a 30% reduced hydrolysis rate in vitro, likely due to the mutation affecting the phosphoryl-binding site in the Rab protein (Walworth et al., 1992). We did not detect any change in expression compared with the wild-type protein (Fig. S2 A). In cells where chromosomal Sec4-Q79L was GFP-tagged, the tethering time of vesicles entering the bud increased 2.5-fold and was far more variable at 45.6 ± 11.7 s (n = 15; Fig. 1, D and E; and Video 2). This implies that the timing of Sec4-GTP hydrolysis occurs before fusion and regulates post-tethering activities of the vesicle. Further analysis of the vesicle-position data showed that the vesicles did not "wander" on the plasma membrane any faster than in wild-type cells, with each moving no more than ∼125 nm/s when tethered to the cortex (Fig. 1 F). There was, however, an eightfold increase in the number of vesicle untethering events in GFP-Sec4-Q79L cells. In these events, the vesicles are tethered to the cortex for several seconds but then are observed untethering in an aborted fusion event (Fig. 1 G and Fig. S2 B). This suggests that a window of opportunity exists for the fusion event to occur, and, if missed, a regulatory mechanism untethers the vesicle for another attempt at an alternate site. The nature of this correction mechanism is unknown. These data, in sum, show that the Sec4-GTP hydrolysis event regulates the tethering time, and if delayed results in an increase of aborted vesicle fusion events.

We next sought to determine how inhibiting certain key steps in exocytosis affects vesicle tethering and fusion at the single-vesicle level. Sec6p is a core member of the exocyst complex involved in both tethering and signaling at fusion sites (TerBush and Novick, 1995; Sivaram et al., 2005; Morgera et al., 2012). Importantly, the exocyst complex becomes disassembled and its function disrupted in the *sec6-4* temperature-sensitive mutant (TerBush and Novick, 1995; Lamping et al., 2005). At the permissive temperature, vesicle tethering times increased to 23.1 ± 5.6 s (n = 16; Fig. 2, A and C). However, these cells showed no difference in vesicle wandering velocity or in aborted tethering events compared with wild type (Fig. 1, F and G), so this minor, but significant, delay likely reflects a defect in a previously unappreciated role in regulating downstream fusion events. Importantly, by examining kymographs of the entire bud cortex, we were unable to detect any

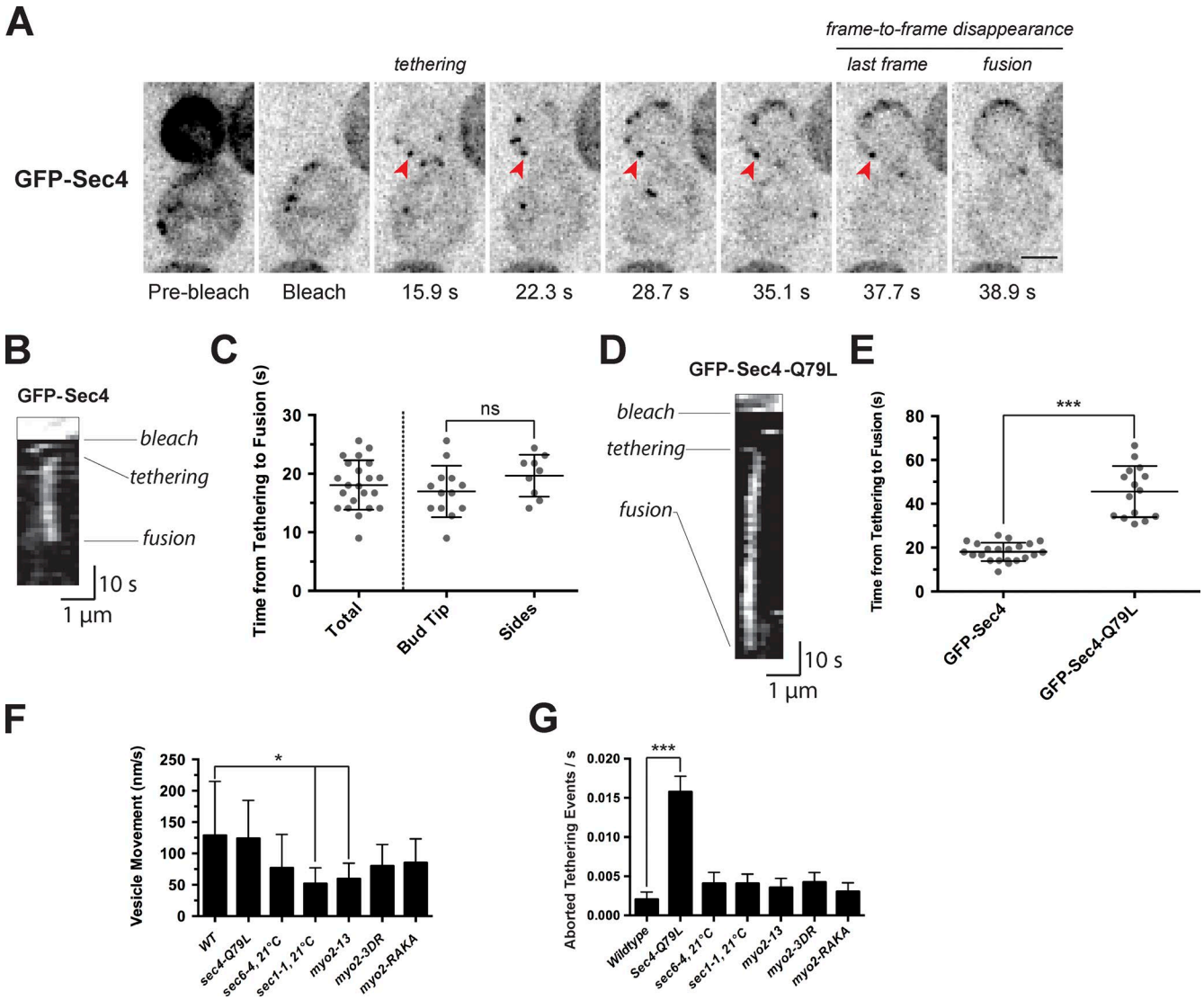

Figure 1. **Vesicles tether to the cortex for ~18 s in wild-type cells, which lengthens and is more variable in a constitutively active Rab mutant.** (A) Still frames of a typical GFP-Sec4 vesicle tracking experiment in a wild-type cell. An inverted monochrome maximum projection is shown for clarity. Arrows point to GFP-Sec4 puncta tethered to the membrane. Bar, 2 µm. See also Video 1 and Fig. S1. (B) Kymograph of GFP-Sec4 vesicle puncta shown by the arrowheads in A. (C) Column scatter plot of the time from tethering to fusion (in seconds) in wild-type cells for the whole population (n = 22), bud tip (n = 13), and bud sides (n = 9). ns, not significant. Lines show mean and 95% confidence intervals. (D) Kymograph of GFP-Sec4-Q79L vesicle puncta. See also Video 2. (E) Column scatter plot of the time from vesicle tethering to fusion (in seconds) in the indicated strains. ***, P < 0.0001. Lines show mean and 95% confidence intervals for wild type (n = 22) and GFP-Sec4-Q79L (n = 15). (F) Movement (nm/s) of puncta tethered to the cortex for the strains indicated at 21°C. Wild type (n = 22), *GFP-Sec4-Q79L* (n = 15), *sec6-4* (n = 16), *sec1-1* (n = 15), *myo2-13* (n = 15), *myo2-3DR* (n = 14), and *myo2-RAKA* (n = 16) are shown. *, P < 0.05. Error bars indicate standard deviation. (G) Aborted tethering events per second for the strains indicated at 21°C. Wild type (n = 22), *GFP-Sec4-Q79L* (n = 15), *sec6-4* (n = 16), *sec1-1* (n = 15), *myo2-13* (n = 15), *myo2-3DR* (n = 14), and *myo2-RAKA* (n = 16) are shown. ***, P < 0.0001. Error bars indicate standard deviation.

lasting vesicle tethering events at the restrictive temperature after a 5-min shift (Fig. 2, D and E). This supports the long-standing hypothesis that the exocyst functions as a physical tether at sites of exocytosis (TerBush and Novick, 1995; Luo et al., 2014), and validates that the tethering we have documented in wild-type cells is mediated by the exocyst.

We next visualized tethering and fusion in a mutant of the SM protein Sec1p, which has been proposed to stimulate assembled SNARE complexes to complete fusion (Scott et al., 2004). The time from tethering to fusion at the permissive temperature was 19.8 ± 5.5 s (n = 15; Fig. 2, B and C), which is not significantly different from wild type. Short 5-min shifts to the restrictive temperature showed that vesicles remained tethered to the cortex, with no clear fusion events being detected (Fig. 2 f). We also did not detect any increase in aborted tethering events at the permissive temperature, but there was a slight decrease in the mobility of the vesicle on the cortex (Fig. 1, f and g). Therefore, when the SM protein is rendered nonfunctional, tethering continues, indicating that the dissociation of the tethering complex requires the function of the SM protein.

The myosin-V Myo2p regulates the time of secretory vesicle tethering

We have described conditional mutations in the cargo-binding domain of the essential myosin-V, Myo2p, that fail to transport

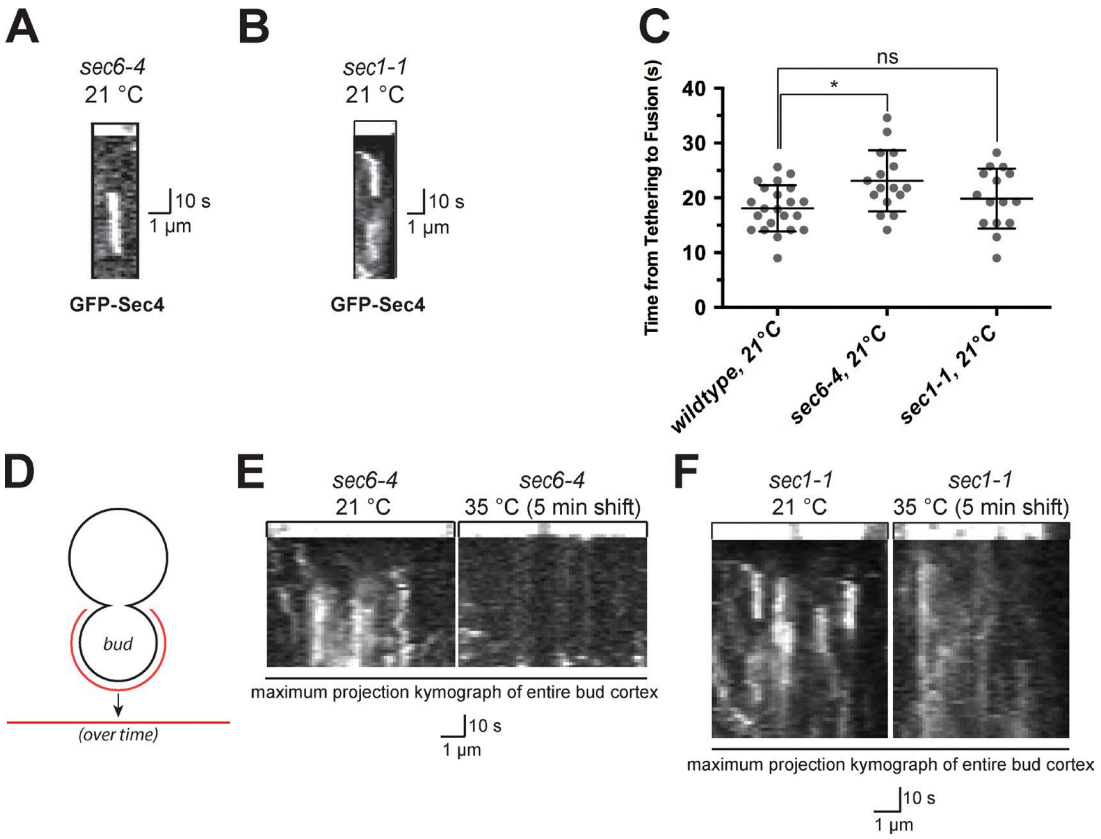

Figure 2. **Vesicle tethering does not occur at the restrictive temperature in *sec6-4* cells, whereas vesicles remain tethered in *sec1-1* cells.** (A) Kymograph of GFP-Sec4 vesicle puncta shown in a *sec6-4* strain at the permissive temperature. (B) Kymograph of GFP-Sec4 vesicle puncta shown in the *sec1-1* strain at the permissive temperature. (C) Column scatter plot of the time from tethering to fusion (in seconds) in wild-type (n = 22), *sec6-4* (n = 16), and *sec1-1* (n = 15) cells at 21°C. *, $P < 0.05$; ns, not significant. Lines show mean and 95% confidence intervals. (D) Schematic diagram for creating kymographs along the entire bud cortex over time. (E) Kymograph of GFP-Sec4 along the entire bud cortex in an *sec6-4* strain at the permissive and restrictive temperature (5 min shift). (F) Kymograph of GFP-Sec4 along the entire bud cortex in an *sec1-1* strain at the permissive and restrictive temperatures (5 min shift).

secretory vesicles at the restrictive temperature (Schott et al., 1999). One of these alleles, *myo2-13*, is misregulated at both the permissive and restrictive temperatures, and is therefore hyperpolarized in the bud, as it has a reduced ability to deactivate (Donovan and Bretscher, 2012). The time of tethering before fusion in the *myo2-13* mutant at the permissive temperature is extended to 27.9 ± 7.5 s (n = 15; Fig. 3, A and D), revealing that a mutant motor protein can influence the vesicle tethering time. This delay may indicate that fusion requires timely release of the motor, or because Myo2p itself participates in a dependent event and the *myo2-13* allele is defective in this function.

To distinguish between these possibilities, we examined tethering in two additional active mutants. We recently showed that Myo2p undergoes a head-to-tail regulatory interaction in vivo through acidic residues in the head and basic residues in the tail; disruption of this interaction renders the motor hyperactive and therefore hyperpolarized in the bud (Donovan and Bretscher, 2015). Analysis of secretory vesicle tethering in two active mutants (*myo2-3DR* and *myo2-RAKA*) shows that they do not enhance the tethering time, indicating that some function other than unregulated motor activity is defective in the *myo2-13* allele (Fig. 3, B–D). One avenue by which the motor might control tethering is through its interaction with exocyst component Sec15p, which was shown to interact with the tail of Myo2p (Jin et al., 2011). However, this interaction is disrupted by the *myo2-RAKA* allele, which indicates that the interaction of Myo2p with Sec15p does not contribute to the extension of the tethering time seen in the *myo2-13* allele. Thus, our data imply that Myo2p contributes to the timing of events during exocytosis, but that the mechanism is unrelated to its state of activation. To this point, our results show that it is possible to follow exocytosis of individual secretory vesicles, and that the time of tethering by the exocyst is influenced by the activity state of Sec4p, an SM protein, and the motor Myo2p that delivered the vesicle.

Myo2 leaves the tethered secretory vesicle 4 s before fusion

Our earlier studies revealed that Myo2p remains associated with secretory vesicles at sites of exocytosis, and that its release requires exocyst complex tethering and Sec4-GTP hydrolysis (Donovan and Bretscher, 2012). To explore the fate of Myo2p present on secretory vesicles during the tethering and fusion steps of exocytosis, we colocalized the vesicle/fusion marker GFP-Sec4 with Myo2-3×mCherry. Myo2p was also present on secretory vesicles during the tethering step as we expected, but disappeared from vesicles ∼4 s before the GFP-Sec4 fusion event (Fig. 4, A and E). In addition, most events showed a gradual tapering of Myo2p intensity on the secretory vesicle before complete disappearance (Fig. 4 B). Because Myo2p's association with vesicles is dependent on Sec4-GTP binding (Santiago-Tirado et al., 2011; Donovan and Bretscher, 2012),

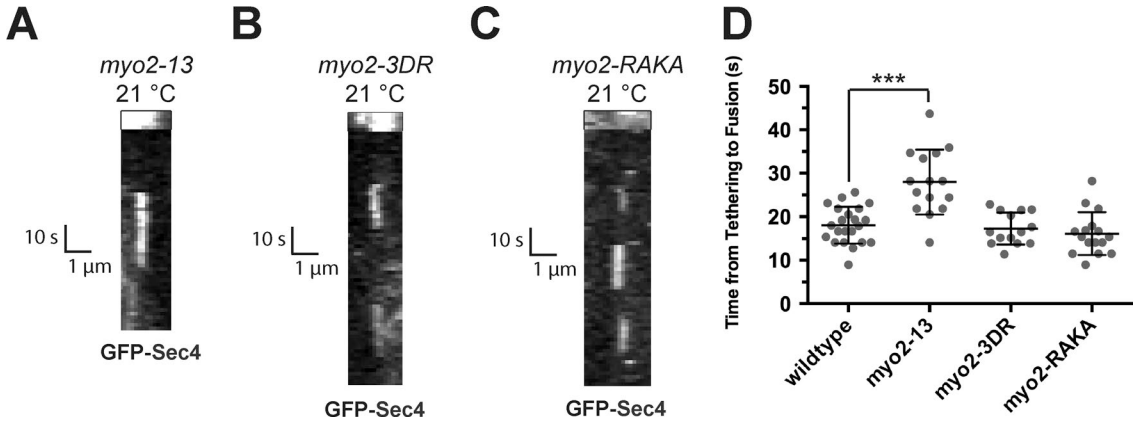

Figure 3. **The myosin-V Myo2p regulates the time of secretory vesicle tethering.** (A) Kymograph of GFP-Sec4 vesicle puncta shown in a *myo2-13* strain at the permissive temperature. (B) Kymograph of GFP-Sec4 vesicle puncta shown in a *myo2-3DR* strain. (C) Kymograph of GFP-Sec4 vesicle puncta shown in a *myo2-RAKA* strain. (D) Column scatter plot of the time from tethering to fusion (in seconds) in wild-type (n = 22), *myo2-13* (n = 15), *myo2-3DR* (n = 14), and *myo2-RAKA* (n = 16) cells at 21°C. ***, $P < 0.0001$; ns, not significant. Lines show mean and 95% confidence intervals.

one explanation for this result is that we are capturing "rolling" Sec4-GTP hydrolysis events of the ∼50 Sec4p molecules on the vesicle from ∼10–4 s before fusion. While we were unable to directly measure Sec4-GTP levels at the fusion site (such as through construction of a probe), it may be that the Sec4-GTP associated with the exocyst or SNARE apparatus is protected from the activity of the Sec4p GAPs Msb3p and Msb4p until a signal triggers fusion.

The GEF Sec2p and the exocyst remain associated with secretory vesicles up to the time of fusion

The GEF Sec2p is associated with secretory vesicles and is critical for the activation of Sec4p necessary for both secretory vesicle transport and binding to the exocyst (Walch-Solimena et al., 1997; Guo et al., 1999). It is not known if Sec2p remains with secretory vesicles during tethering, as it might dissociate to allow inactivation of Sec4-GTP by GAPs Msb3/4p (Gao et al., 2003). It was therefore of considerable interest to see at which point Sec2p leaves secretory vesicles. In a strain with chromosomally tagged GFP-Sec4 and Sec2-3×mCherry, Sec2p was found to remain associated with secretory vesicles up to the point of fusion (Fig. 4, C and E). This may indicate that the GEF is required for some portion of the fusion event, such as keeping some of the pool of vesicle-localized Sec4p in a GTP-bound state or regulating the exocyst complex through its interaction with Sec15p (Mizuno-Yamasaki et al., 2010; Stalder et al., 2013).

Sec4-GTP hydrolysis has been postulated to regulate several events at the bud cortex, including its association with Myo2p and the exocyst, as well as regulating proper SNARE assembly (Guo et al., 1999; Grosshans et al., 2006; Santiago-Tirado et al., 2011; Donovan and Bretscher, 2012). Exocyst component Sec15p directly binds to Sec4p in a GTP-dependent manner and has been proposed to link the rest of the exocyst complex to the vesicle (Guo et al., 1999). We were able to detect some Sec4p/Sec15p colocalization on vesicles in the mother cell, but did not detect significant Sec4p or exocyst component overlap with the trans-Golgi marker Sec7p; this is consistent with the model that at least some components of the exocyst complex load onto vesicles before transport (Boyd et al., 2004; Fig. S3).

In contrast to Myo2p, Sec15-3×mCherry appeared to leave at the moment GFP-Sec4 disappears, which implies it is leaving at the fusion event (Fig. 4, D and E). This was intriguing because the Rab's interactions with both Myo2p and Sec15p are regulated by GTP hydrolysis; however, as the exocyst is essential for exocytosis, it is conceivable that Sec15p must be present at sites of fusion until the end of the event. Further, the exocyst is well integrated to plasma membrane–localized Rho proteins Rho1p, Rho3p, and Cdc42p (Robinson et al., 1999; Guo et al., 2001; Zhang et al., 2001) and Sec2p via a phosphoryl regulation (Stalder et al., 2013), both of which may keep it from freely diffusing away. Our data showing that Sec15p remains with the vesicle until fusion are also similar to a recent observation in a mammalian vesicle fusion study, which found that the exocyst component Sec8 is present on vesicles at fusion sites but then leaves ∼2 s after vesicle fusion (Rivera-Molina and Toomre, 2013).

The exocyst is a nearly megadalton complex, with dimensions of 13 × 30 nm in a closed form (Hsu et al., 1998). As Sec15p is found on vesicles right up to the moment of fusion, this suggests that the complex must either disassemble or rearrange to accommodate the fusion of the 80-nm secretory vesicle. To better understand this result, we explored the behavior of additional exocyst complex components. We chose to tag Sec3p because it physically contacts the cortex through Rho proteins, and Sec5p because it is present on secretory vesicles but does not contact Sec15p (Guo et al., 1999, 2001; Zhang et al., 2001). In both cases, exocyst components left secretory vesicles at the same time as Sec15p, suggesting that the exocyst does not disassemble before fusion and may instead rearrange to accommodate vesicle fusion (Fig. 4, F–H). Additional evidence that the exocyst does not disassemble before fusion comes from fluorescence loss in photobleaching (FLIP) experiments, in which the mother cell is continuously bleached and the fluorescence intensity of protein in the bud is monitored over time; thus, the relative rates of recycling from the bud can be compared for different proteins. All exocyst proteins were observed to recycle from the bud at similar rates (Fig. 4 I), with ∼70% of the population for all components being in the mobile fraction. This suggests that the exocyst complex recycles from the bud as a single unit and therefore must later break up into "v-exocyst" and "t-exocyst" components for another round of tethering.

Despite thirty years of work dissecting post-Golgi secretion in budding yeast, the precise temporal localizations of dif-

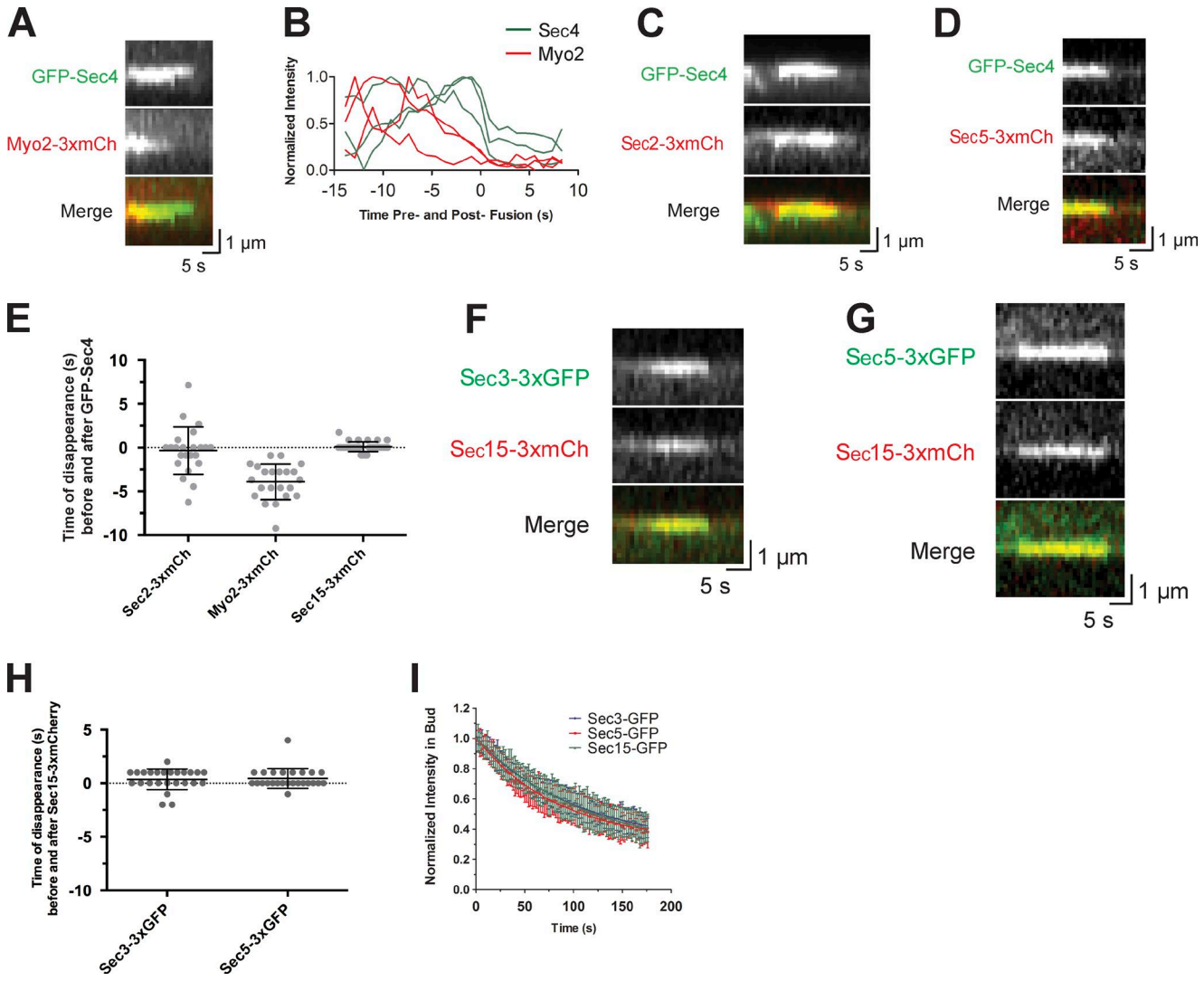

Figure 4. **Myo2p dissociates from the vesicle ∼4 s before fusion while the GEF Sec2p and exocyst components dissociate at the fusion event.** (A) Kymographs of GFP-Sec4 and Myo2-3×mCherry puncta during the fusion event. Note the gradual decrease in intensity of Myo2-3×mCherry before its complete disappearance. (B) Line scans of three different kymograph traces showing Myo2-3×mCherry leaving a vesicle gradually before the fusion event at t = 0 s. Intensity was normalized. (C) Kymographs of GFP-Sec4 and Sec2-3×mCherry puncta during the fusion event. (D) Kymographs of GFP-Sec4 and Sec15-3×mCherry puncta during the fusion event. (E) Column scatter plot of the time of disappearance (in seconds) for the protein of interest compared with the fusion event (GFP-Sec4 disappearance). Sec2-3×mCherry, *n* = 23; Myo2-3×mCherry, *n* = 22; Sec15-3×mCherry, *n* = 30. Lines show mean and 95% confidence intervals. (F) Kymographs of Sec3-3×GFP and Sec15-3×mCherry puncta during the fusion event. (G) Kymographs of Sec5-3×GFP and Sec15-3×mCherry puncta during the fusion event. (H) Column scatter plot of the time of disappearance (in seconds) for Sec3p or Sec5p compared with the fusion event (Sec15p disappearance). *n* = 25 for both datasets. Lines show mean and 95% confidence intervals. (I) FLIP experiments showing the normalized intensity in the bud for tagged exocyst components. Best-fit curves were single-exponential decay with one rate of loss from the bud. Half times of loss from the bud were 71.0 ± 9.4 s (Sec3-GFP, *n* = 15), 58.1 ± 9.4 s (Sec5-GFP; *n* = 13), and 78.2 ± 17.1 s (Sec15-GFP; *n* = 10). Error bars indicate standard deviation.

ferent components at the cell cortex during exocytosis has not been achieved until now. A timeline of events summarizing our results is presented in Fig. 5. Several interesting questions are raised by this analysis. It is tempting to speculate that the Rab hydrolysis event is the master timing control for vesicle fusion given the delay between wild-type and hydrolysis-impaired mutants, though this could be due to other factors such as the mutant impairing SNARE assembly. Further, it is striking to see just how immobile tethered vesicles are on the plasma membrane, and we cannot offer an explanation for this phenomenon. As the proteins tracked in this study are highly conserved through evolution, these results are likely widely applicable. This study sets the stage, using additional mutants and altering the levels of key components, to fully dissect these events and establish how vesicle tethering, motor release, GTP hydrolysis, and membrane fusion events are coordinated, corrected, and timed.

Materials and methods

Yeast strains and constructs

Cells were grown and selected for using standard molecular biology techniques (Sherman, 2002). Yeast transformations were performed using lithium acetate–based methods (Gietz et al., 1995). In brief, log phase cultures were transformed for 45 min at 42°C with the vector/PCR product in a mixture of ∼40% wt/vol PEG-3350 (Sigma-Aldrich), 0.1 M lithium acetate (Sigma-Aldrich), and 0.28 mg/ml SS carrier DNA (Sigma-Aldrich). Transformants were always

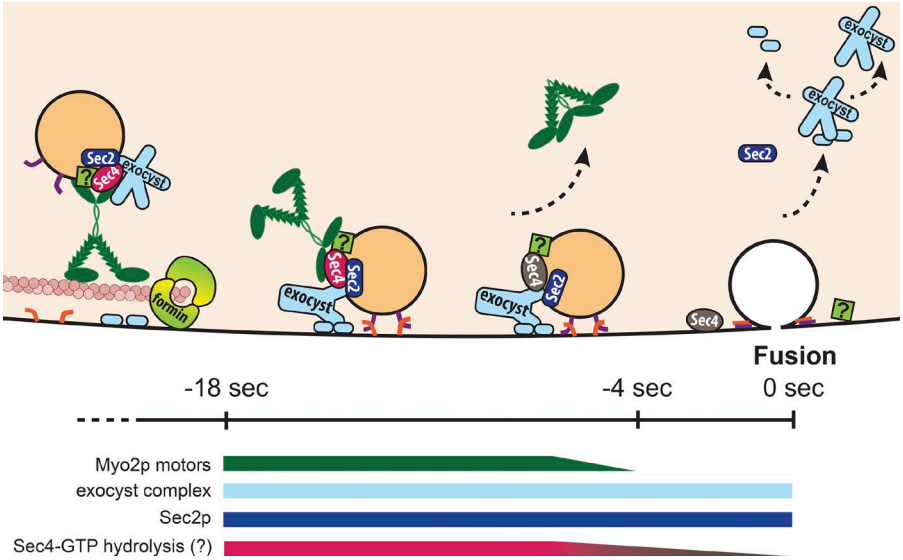

Figure 5. **A timeline of events during yeast exocytosis.** Several Myo2p motors (one is shown for simplicity) transport a vesicle to sites of exocytosis via interactions with Sec4p, the exocyst (through Sec15p), and an unknown component interacting with PI4P (shown with a question mark). Vesicle tethering via the exocyst complex physically attaches the vesicle to the cortex, which lasts for 18 s in wild-type cells. Myo2p motors are released gradually, with all dissociated ∼4 s before fusion. This may indicate that Sec4-GTP is also hydrolyzed on a continuum. Finally, the GEF Sec2p and the exocyst complex are released at the moment of vesicle fusion, which then likely breaks into vesicle-associated and plasma membrane–associated components for another round of tethering. Not shown is the recycling event of the SNARE proteins, Sec4p by GDI, or the recycling of the unknown component of the receptor complex.

selected for on appropriate synthetic media. Table S1 shows the strains used in this study.

DNA constructs

GFP-Sec4 was chromosomally integrated into strains using the endogenous promoter and locus (Donovan and Bretscher, 2012). In brief, this vector contains 400 nt of the *SEC4* promoter, followed by *GFP*, *SEC4*, and the *SEC4* terminator. Colocalization experiments were performed with either 3×GFP or 3×mCherry fused to the C terminus of the protein of interest. All PCR-amplified fragments were sequenced after ligation to ensure fidelity. Myo2-3×mCherry was created by removing a 3×GFP module from pRS306-cctail-3×GFP and ligating a 3×mCherry module between the BamHI and NotI restriction sites. The vector was then cut with a unique HindIII site for integration at the 3′ end of the endogenous *MYO2* gene. Strains containing Sec15-3×mCherry were created by ligating a PCR-amplified fragment of the 3′ end of *SEC15* (1,008 nt) between restriction sites HindIII and BamHI in the pRS306 vector. A 681-nt fragment of the *SEC15* 3′ untranslated region was ligated upstream, between XhoI and HindIII, while the 200 nt fragment of the *SEC15* terminator was amplified and ligated between the SacI and NotI sites. After ligation of the 3×mCherry module between BamHI and NotI, the construct was linearized with the unique HindIII site to integrate 3×mCherry immediately 3′ of the *SEC15* gene. A similar strategy was done for Sec2-3×mCherry, using a unique SpeI cut site to linearize and integrate. Sec3p and Sec5p were tagged with 3×GFP by amplifying the 3′ 1,000 nt of each gene sequence and ligating into a pRS303-3×GFP-tADH1 construct between the BamHI and SalI restriction sites. Each gene fragment has a unique ClaI restriction site; when linearized, 3×GFP integrated at the 3′ end of the gene in question. The plasmid pSSEC7-DsRed.M1 × 6, which contains *SEC7* driven from the *TPI1* promoter followed by six tandem dsRed genes, was a gift from the B. Glick laboratory (University of Chicago, Chicago, IL). The CEN plasmid used in GFP-Ypt31 studies was a gift from the R. Collins laboratory (Cornell University, Ithaca, NY) and contains the endogenous promoter. The plasma membrane marker used in our control experiments was the CEN plasmid pRS415-pTOM3-mCherry (2X Ist2$^{928–948}$), a gift from the S. Emr laboratory (Cornell University).

Exocyst components used in FLIP photobleaching were tagged with GFP by amplifying PCR cassettes from pFA6a-GFP vectors and selected for using the appropriate media (Longtine et al., 1998). Hyperactive mutants *myo2-3DR* (D123R/E135R/E137R) and *myo2-RAKA* (R1402A/K1473A) were integrated into the chromosome as the sole copy (Donovan and Bretscher, 2015). In brief, site-directed mutagenesis was performed on constructs containing the region −500 to +750 of the *MYO2* head domain, or nucleotides 3272–4725 of *MYO2*. Note that the *myo2-RAKA* allele mutates the same residues as the *myo2-REKE* allele used in a different study (Donovan and Bretscher, 2015), except that the basic patch on the tail was mutated to alanine instead of glutamic acid. There is no change in phenotype.

Vesicle tethering assay

"Vesicles" in this assay are defined as GFP-Sec4–positive puncta. All assays were done in strains grown to mid-log phase in appropriate synthetic media containing dextrose. Live cell imaging of log-phase cells was performed at 21°C or after a 5-min shift to 35°C where appropriate. Cells were imaged on a 35-mm MatTek dish (Ashland) pretreated with 0.05 mg/ml Concanavalin A (EY Laboratories, Inc.).

Micrographs were taken on a spinning disc confocal microscope system (CSU-X; Intelligent Imaging Innovations) using an inverted microscope (DMI600B; Leica) and a camera (CoolSnap HQ2; Photometrics). Micrographs were captured using the 100×/1.46 NA objective lens with 2× binning, for an effective pixel resolution of ∼14 nm^2. Movies were taken in a z stack of 5 planes (covering 2.5 µm), each with 150-ms exposure times from a 488-nm laser, for a time resolution of ∼1.32 s per frame. This allows for the capture of about half of the bud in late G2 phase. Photobleaching of the entire bud was performed using a Vector photomanipulation system (Intelligent Imaging Innovations) with a 1-ms dwell time and a raster block size of 10.

GFP-Sec4–positive vesicles entering the bud after FRAP were tracked in three dimensions in Slidebook 5.0 using the "Mean Adjusted Center of Intensity" manual particle tracking tool. This finds the coordinates of the center of the object (weighted by intensity values that are above the mean intensity). Vesicles were tracked by eye until one was observed tethering to the membrane. The manual particle tracker tool was then used to measure the particle's location in 3D space of the multiplaned image until it disappeared. Only those vesicles that contacted the membrane from the cytoplasm, were unambiguous throughout their time there (that is, no other vesicle appeared next to it or overlapped with it), and quickly vanished in the middle three planes of the five plane image were used. This last criterion was included to prevent sampling vesicles that might drift out of the field of view in the z direction. Statistics related to the path of the vesicle were then obtained from Slidebook 5.0 and exported for work in Microsoft Excel and GraphPad Prism. Aborted tethering events for different strains were scored as the

vesicles that dissociated from the cortex after being tethered for at least four consecutive frames (~5 s) of 20 separate movies. Imaging projections were also created in Slidebook 5.0.

Colocalization experiments

Colocalization microscopy of tethered Sec4p, Myo2p, Sec15p, Sec3p, and Sec5p was performed by imaging a single bottom plane of the cell. This was done to increase time resolution to <1 s, and because it was found that tethered vesicles in wild-type cells are relatively immobile on the plasma membrane (Fig. 1 G). GFP-Sec4 channel was captured for 120 ms per frame while the 3×mCherry-tagged protein was captured for 750 ms per frame. For exocyst component colocalization, Sec15-3×mCherry was captured for 500 ms while either Sec3-3×GFP or Sec5-3×GFP were captured for 400 ms. The times of disappearance for proteins analyzed were calculated by observing movie frames and comparing time stamps. Colocalization of GFP-Ypt31 and Sec7-6×dsRed in the mother cell was performed for the indicated strains at different exposure times as needed. FLIP photobleaching experiments were performed by imaging the cell every 2 s while photobleaching the mother cell every 6 s using the Vector control system (Intelligent Imaging Innovations) with 1 ms dwell time and a raster block size of 20.

Western blotting

Log phase cell cultures were washed once in ice-cold water, spun down, and resuspended in 1× Laemmli sample buffer. 4 × 1 min bead disruption was then done to break open the cells, with 1 min on ice in between runs. Samples were then boiled for 30 s at 95°C and resolved on a 12% SDS-PAGE gel. After transfer and blocking, membranes were probed with anti-Sec4p (generated in rabbit against full-length Sec4p missing its CAX box motif) and loading control anti-Zwf1p (also known as the G6PDH enzyme; generated in rabbit against the full-length protein).

Statistics

Student's *t* test and one-way analysis of variance (ANOVA) were used to determine statistical significance between datasets. A 95% confidence interval ($P < 0.05$) was considered significant.

Online supplemental material

Fig. S1 shows control bleach experiments and colocalization between GFP-Sec4–marked vesicles and a plasma membrane marker. Fig. S2 provides protein expression control blots and an example of an aborted tethering event from the GFP-Sec4-Q79L analysis. Fig. S3 shows colocalization data for Rab proteins, the trans-Golgi network protein Sec7p, and exocyst components. Videos 1 and 2 show examples of bleached cells used in vesicle tracking studies for wild-type GFP-Sec4 and GFP-Sec4-Q79L strains, respectively. Table S1 shows the strains used in this study. Online supplemental material is available at http://www.jcb.org/cgi/content/full/jcb.201501118/DC1.

Acknowledgements

We would like to thank members of the Bretscher laboratory for helpful discussions and for reading this manuscript. We also thank C. Boone, E. Bi, P. Novick, R. Collins, B. Glick, and S. Emr for strains and constructs used in this study.

This work was supported by the National Institutes of Health (grant GM39066).

The authors declare no competing financial interests.

Author contributions: K.W. Donovan designed and performed experiments and contributed to the manuscript. A. Bretscher designed experiments and contributed to the manuscript.

Submitted: 29 January 2015
Accepted: 15 June 2015

References

Boyd, C., T. Hughes, M. Pypaert, and P. Novick. 2004. Vesicles carry most exocyst subunits to exocytic sites marked by the remaining two subunits, Sec3p and Exo70p. *J. Cell Biol.* 167:889–901. http://dx.doi.org/10.1083/jcb.200408124

Brennwald, P., and G. Rossi. 2007. Spatial regulation of exocytosis and cell polarity: yeast as a model for animal cells. *FEBS Lett.* 581:2119–2124. http://dx.doi.org/10.1016/j.febslet.2007.03.043

Carr, C.M., E. Grote, M. Munson, F.M. Hughson, and P.J. Novick. 1999. Sec1p binds to SNARE complexes and concentrates at sites of secretion. *J. Cell Biol.* 146:333–344. http://dx.doi.org/10.1083/jcb.146.2.333

D'Adamo, P., A. Menegon, C. Lo Nigro, M. Grasso, M. Gulisano, F. Tamanini, T. Bienvenu, A.K. Gedeon, B. Oostra, S.-K. Wu, et al. 1998. Mutations in GDI1 are responsible for X-linked non-specific mental retardation. *Nat. Genet.* 19:134–139. http://dx.doi.org/10.1038/487

Donovan, K.W., and A. Bretscher. 2012. Myosin-V is activated by binding secretory cargo and released in coordination with Rab/exocyst function. *Dev. Cell.* 23:769–781. http://dx.doi.org/10.1016/j.devcel.2012.09.001

Donovan, K.W., and A. Bretscher. 2015. Head-to-tail regulation is critical for the in vivo function of myosin V. *J. Cell Biol.* 209:359–365. http://dx.doi.org/10.1083/jcb.201411010

Evangelista, M., D. Pruyne, D.C. Amberg, C. Boone, and A. Bretscher. 2002. Formins direct Arp2/3-independent actin filament assembly to polarize cell growth in yeast. *Nat. Cell Biol.* 4:32–41. (Corrected and republished in *Nat. Cell Biol.* 2002. 4:260–269) http://dx.doi.org/10.1038/ncb718

Gao, X.-D., S. Albert, S.E. Tcheperegine, C.G. Burd, D. Gallwitz, and E. Bi. 2003. The GAP activity of Msb3p and Msb4p for the Rab GTPase Sec4p is required for efficient exocytosis and actin organization. *J. Cell Biol.* 162:635–646. http://dx.doi.org/10.1083/jcb.200302038

Gietz, R.D., R.H. Schiestl, A.R. Willems, and R.A. Woods. 1995. Studies on the transformation of intact yeast cells by the LiAc/SS-DNA/PEG procedure. *Yeast.* 11:355–360. http://dx.doi.org/10.1002/yea.320110408

Grosshans, B.L., A. Andreeva, A. Gangar, S. Niessen, J.R. Yates III, P. Brennwald, and P. Novick. 2006. The yeast lgl family member Sro7p is an effector of the secretory Rab GTPase Sec4p. *J. Cell Biol.* 172:55–66. http://dx.doi.org/10.1083/jcb.200510016

Guo, W., D. Roth, C. Walch-Solimena, and P. Novick. 1999. The exocyst is an effector for Sec4p, targeting secretory vesicles to sites of exocytosis. *EMBO J.* 18:1071–1080. http://dx.doi.org/10.1093/emboj/18.4.1071

Guo, W., F. Tamanoi, and P. Novick. 2001. Spatial regulation of the exocyst complex by Rho1 GTPase. *Nat. Cell Biol.* 3:353–360. http://dx.doi.org/10.1038/35070029

Hsu, S.-C., C.D. Hazuka, R. Roth, D.L. Foletti, J. Heuser, and R.H. Scheller. 1998. Subunit composition, protein interactions, and structures of the mammalian brain sec6/8 complex and septin filaments. *Neuron.* 20:1111–1122. http://dx.doi.org/10.1016/S0896-6273(00)80493-6

Jin, Y., A. Sultana, P. Gandhi, E. Franklin, S. Hamamoto, A.R. Khan, M. Munson, R. Schekman, and L.S. Weisman. 2011. Myosin V transports secretory vesicles via a Rab GTPase cascade and interaction with the exocyst complex. *Dev. Cell.* 21:1156–1170. http://dx.doi.org/10.1016/j.devcel.2011.10.009

Johnston, G.C., J.A. Prendergast, and R.A. Singer. 1991. The *Saccharomyces cerevisiae* MYO2 gene encodes an essential myosin for vectorial transport of vesicles. *J. Cell Biol.* 113:539–551. http://dx.doi.org/10.1083/jcb.113.3.539

Lamping, E., K. Tanabe, M. Niimi, Y. Uehara, B.C. Monk, and R.D. Cannon. 2005. Characterization of the *Saccharomyces cerevisiae* sec6-4 mutation and tools to create *S. cerevisiae* strains containing the sec6-4 allele. *Gene.* 361:57–66. http://dx.doi.org/10.1016/j.gene.2005.07.014

Lehman, K., G. Rossi, J.E. Adamo, and P. Brennwald. 1999. Yeast homologues of tomosyn and lethal giant larvae function in exocytosis and are associated with the plasma membrane SNARE, Sec9. *J. Cell Biol.* 146:125–140. http://dx.doi.org/10.1083/jcb.146.1.125

Lillie, S.H., and S.S. Brown. 1994. Immunofluorescence localization of the unconventional myosin, Myo2p, and the putative kinesin-related protein, Smy1p, to the same regions of polarized growth in *Saccharomyces cerevisiae*. *J. Cell Biol.* 125:825–842. http://dx.doi.org/10.1083/jcb.125.4.825

Liu, H.P., and A. Bretscher. 1989. Disruption of the single tropomyosin gene in yeast results in the disappearance of actin cables from the cytoskeleton. *Cell.* 57:233–242. http://dx.doi.org/10.1016/0092-8674(89)90961-6

Longtine, M.S., A. McKenzie III, D.J. Demarini, N.G. Shah, A. Wach, A. Brachat, P. Philippsen, and J.R. Pringle. 1998. Additional modules for versatile and economical PCR-based gene deletion and modification in *Saccharomyces cerevisiae*. *Yeast.* 14:953–961. http://dx.doi.org/10.1002/(SICI)1097-0061(199807)14:10<953::AID-YEA293>3.0.CO;2-U

Luo, G., J. Zhang, and W. Guo. 2014. The role of Sec3p in secretory vesicle targeting and exocyst complex assembly. *Mol. Biol. Cell.* 25:3813–3822. http://dx.doi.org/10.1091/mbc.E14-04-0907

Mizuno-Yamasaki, E., M. Medkova, J. Coleman, and P. Novick. 2010. Phosphatidylinositol 4-phosphate controls both membrane recruitment and a regulatory switch of the Rab GEF Sec2p. *Dev. Cell.* 18:828–840. http://dx.doi.org/10.1016/j.devcel.2010.03.016

Morgera, F., M.R. Sallah, M.L. Dubuke, P. Gandhi, D.N. Brewer, C.M. Carr, and M. Munson. 2012. Regulation of exocytosis by the exocyst subunit Sec6 and the SM protein Sec1. *Mol. Biol. Cell.* 23:337–346. http://dx.doi.org/10.1091/mbc.E11-08-0670

Novick, P., and R. Schekman. 1983. Export of major cell surface proteins is blocked in yeast secretory mutants. *J. Cell Biol.* 96:541–547. http://dx.doi.org/10.1083/jcb.96.2.541

Novick, P., C. Field, and R. Schekman. 1980. Identification of 23 complementation groups required for post-translational events in the yeast secretory pathway. *Cell.* 21:205–215. http://dx.doi.org/10.1016/0092-8674(80)90128-2

Ortiz, D., M. Medkova, C. Walch-Solimena, and P. Novick. 2002. Ypt32 recruits the Sec4p guanine nucleotide exchange factor, Sec2p, to secretory vesicles; evidence for a Rab cascade in yeast. *J. Cell Biol.* 157:1005–1016. http://dx.doi.org/10.1083/jcb.200201003

Rivera-Molina, F., and D. Toomre. 2013. Live-cell imaging of exocyst links its spatiotemporal dynamics to various stages of vesicle fusion. *J. Cell Biol.* 201:673–680. http://dx.doi.org/10.1083/jcb.201212103

Robinson, N.G., L. Guo, J. Imai, A. Toh-E, Y. Matsui, and F. Tamanoi. 1999. Rho3 of *Saccharomyces cerevisiae*, which regulates the actin cytoskeleton and exocytosis, is a GTPase which interacts with Myo2 and Exo70. *Mol. Cell. Biol.* 19:3580–3587.

Rossi, G., and P. Brennwald. 2011. Yeast homologues of lethal giant larvae and type V myosin cooperate in the regulation of Rab-dependent vesicle clustering and polarized exocytosis. *Mol. Biol. Cell.* 22:842–857. http://dx.doi.org/10.1091/mbc.E10-07-0570

Salminen, A., and P.J. Novick. 1987. A ras-like protein is required for a post-Golgi event in yeast secretion. *Cell.* 49:527–538. http://dx.doi.org/10.1016/0092-8674(87)90455-7

Santiago-Tirado, F.H., A. Legesse-Miller, D. Schott, and A. Bretscher. 2011. PI4P and Rab inputs collaborate in myosin-V-dependent transport of secretory compartments in yeast. *Dev. Cell.* 20:47–59. http://dx.doi.org/10.1016/j.devcel.2010.11.006

Schott, D., J. Ho, D. Pruyne, and A. Bretscher. 1999. The COOH-terminal domain of Myo2p, a yeast myosin V, has a direct role in secretory vesicle targeting. *J. Cell Biol.* 147:791–808. http://dx.doi.org/10.1083/jcb.147.4.791

Schott, D.H., R.N. Collins, and A. Bretscher. 2002. Secretory vesicle transport velocity in living cells depends on the myosin-V lever arm length. *J. Cell Biol.* 156:35–40. http://dx.doi.org/10.1083/jcb.200110086

Scott, B.L., J.S. Van Komen, H. Irshad, S. Liu, K.A. Wilson, and J.A. McNew. 2004. Sec1p directly stimulates SNARE-mediated membrane fusion in vitro. *J. Cell Biol.* 167:75–85. http://dx.doi.org/10.1083/jcb.200405018

Sherman, F. 2002. Getting started with yeast. *Methods Enzymol.* 350:3–41.

Sivaram, M.V.S., J.A. Saporita, M.L.M. Furgason, A.J. Boettcher, and M. Munson. 2005. Dimerization of the exocyst protein Sec6p and its interaction with the t-SNARE Sec9p. *Biochemistry.* 44:6302–6311. http://dx.doi.org/10.1021/bi048008z

Stalder, D., E. Mizuno-Yamasaki, M. Ghassemian, and P.J. Novick. 2013. Phosphorylation of the Rab exchange factor Sec2p directs a switch in regulatory binding partners. *Proc. Natl. Acad. Sci. USA.* 110:19995–20002. http://dx.doi.org/10.1073/pnas.1320029110

TerBush, D.R., and P. Novick. 1995. Sec6, Sec8, and Sec15 are components of a multisubunit complex which localizes to small bud tips in *Saccharomyces cerevisiae*. *J. Cell Biol.* 130:299–312. http://dx.doi.org/10.1083/jcb.130.2.299

Togneri, J., Y.-S. Cheng, M. Munson, F.M. Hughson, and C.M. Carr. 2006. Specific SNARE complex binding mode of the Sec1/Munc-18 protein, Sec1p. *Proc. Natl. Acad. Sci. USA.* 103:17730–17735. http://dx.doi.org/10.1073/pnas.0605448103

Walch-Solimena, C., R.N. Collins, and P.J. Novick. 1997. Sec2p mediates nucleotide exchange on Sec4p and is involved in polarized delivery of post-Golgi vesicles. *J. Cell Biol.* 137:1495–1509. http://dx.doi.org/10.1083/jcb.137.7.1495

Walworth, N.C., P. Brennwald, A.K. Kabcenell, M. Garrett, and P. Novick. 1992. Hydrolysis of GTP by Sec4 protein plays an important role in vesicular transport and is stimulated by a GTPase-activating protein in Saccharomyces cerevisiae. *Mol. Cell. Biol.* 12:2017–2028.

Zhang, X., E. Bi, P. Novick, L. Du, K.G. Kozminski, J.H. Lipschutz, and W. Guo. 2001. Cdc42 interacts with the exocyst and regulates polarized secretion. *J. Biol. Chem.* 276:46745–46750. http://dx.doi.org/10.1074/jbc.M107464200

Zhao, C., J. Takita, Y. Tanaka, M. Setou, T. Nakagawa, S. Takeda, H.W. Yang, S. Terada, T. Nakata, Y. Takei, et al. 2001. Charcot-Marie-Tooth disease type 2A caused by mutation in a microtubule motor KIF1Bbeta. *Cell.* 105:587–597. http://dx.doi.org/10.1016/S0092-8674(01)00363-4